ON THE PERFORMANCE ANALYSIS OF ORGANIC/HYBRID SOLAR CELLS THROUGH RELIABLE PARAMETER EXTRACTION

Constantin DUMITRU[1], Vlad-Florin MUSCUREL[1], Laurentiu FARA[2],

Abstract. *An analysis of three mathematical models of advanced solar cells was developed in order to evaluate and optimize device performance. We have considered the parameter extraction for specific experimental data for performance evaluation [1-4]. The following specific parameters: PCE (power conversion efficiency) I_{sc} (short circuit current), V_{oc} (open circuit voltage) and FF (fill factor) were discussed. This methodology could be used for performance optimization and a way to compare the simulated results with the experimental ones.*

Keywords: organic photovoltaics, parameter extraction, bulk heterojunction solar cell, polymeric materials

1. Introduction

Organic solar cells (OPV) represent a field in constant evolution and rapid development [1] for polymer photovoltaics due to their advantages, like the low production cost in high volumes, good optical absorption and flexibility, (Figure 1,a). State of the art leading conversion efficiency has been reported by Heliatek and confirmed by Fraunhofer-CSP at 13.2% for a multi-junction cell with an active layer comprised of 3 patented absorbers that cover green, red and near-Ir spectrum. Reliable parameter extraction is in demand as standardized methods for OPV comparison and performance optimization [2, 26] use parameter extraction via raw *I-V* data and numerical simulation. An analysis of three mathematical models of advanced solar cells was developed in order to evaluate and optimize device performance. Respectively, the first algorithm uses a Lambert function model which should be very precise with the analytical solution [3], the second one is a double fit model [4-6, 12], which should be faster, and the third algorithm makes use of a linear regression model [7, 27-30]. We have considered the parameter extraction for specific experimental data for performance evaluation The following specific parameters: PCE (power conversion efficiency) I_{sc} (short circuit current), V_{oc} (open circuit voltage) and FF (fill factor) were discussed. This methodology could be used for performance optimization and a way to compare the simulated results with the experimental ones.

[1]Eng., Faculty of Applied Sciences, University "Politehnica" of Bucharest, Physics Department, Academic Centre for Optical Engineering and Photonics, Bucharest, Romania, (condumitru@yahoo.com).
[2]Academy of Romanian Scientists, Bucharest, Romania.

The second section is a discussion on the OPV architecture. In the third section, implementation in both device and model is discussed. The fourth section comments on the accuracy and results comparison between models used for the OPV parameter extraction in this article. The final section is reserved for conclusions from this work.

2. Basic processes

Bulk heterojunction devices, in which photoactive hole carrying polymers phase and electron carrying phase separate at the mesoscopic range are particularly attractive due to their balance of conversion efficiency and low manufacturing costs and are projected to become economically viable above 10% conversion efficiency.

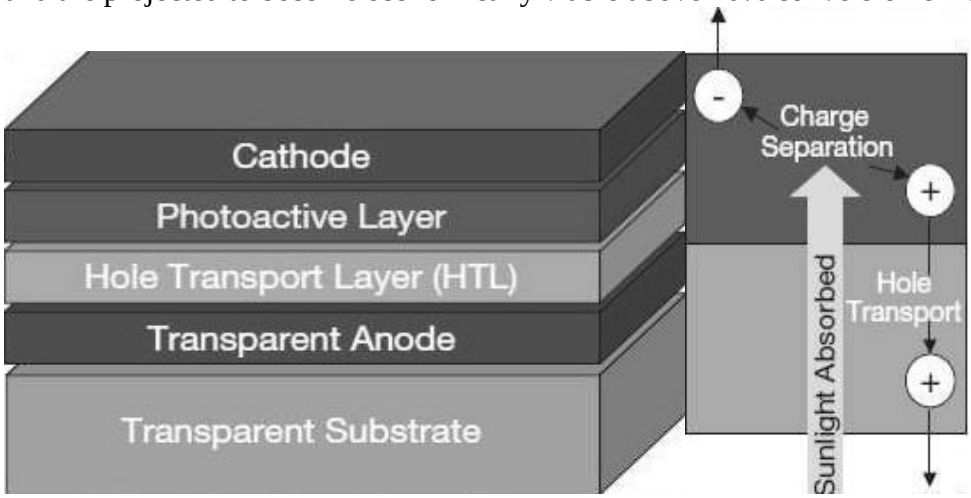

Fig.1. Organic solar cell structure [7].

The processes that govern organic photovoltaics can be summarized as follows (see Figure 1,b):

A. photon absorption and exciton generation

B. charge carrier separation,

C. electron and hole transport

D. charge collection.

Bulk heterojunction devices [8,9], in which photoactive hole carrying polymer phase and electron carrying phase separate at the mesoscopic range are particularly attractive due to their balance of conversion efficiency and low manufacturing costs. Once a photon absorption [10-13] occurs, an electron is excited from the highest occupied molecular orbital (HOMO) to the lowest unoccupied molecular orbital (LUMO). The electron hole pair then relaxes with a binding energy between 0.3–1.4 eV [14,28]. This is different for inorganic materials, where the exciton

energy is only a few milli-electron volts. This binding energy is larger in organic semiconductors because the charge carrier's wave functions are localized and the dielectric constants are small, thus increasing the Coulomb force between the charge carriers. The excitons must then move to an interface phase where there is enough chemical potential energy drops to enable dissociation into an electron hole that spans the interface across the donor and acceptor. The most common structure that allows exciton separation is a planar heterojunction sandwiched between a transparent conductive layer such as indium-tin-oxide (ITO) coated with poly(3,4-ethylenedioxythiophene):poly(styrene sulfonate) (PEDOT:PSS) or fluorinated tin oxide (FTO), and a reflecting metal, such as Ag or Al. The so called internal junction field will disassociate the charged pair formed after exciton split. Afterwards, each charge carrier is transported to the electrodes by drift effect (caused by the internal field) towards the junction charge area, and by means of diffusion to the neutral regions. The current that reaches the contacts with no applied field is known as the short circuit current, I_{sc} or J_{sc}, and the maximum potential generated by the device is known as the Voc namely, the open circuit voltage. The ratio between the maximum power generated and the product of Voc and Isc is known as the fill factor, and is closely connected to the quality of the OPV device. The efficiency of the planar heterojunction device is limited by the exciton diffusion length. The distance which excitons travel before recombination happens and is roughly 3–10 nm in most organic semiconductors.

That means the active volume of this subtype of solar cell is limited to a very small length region close to the interface, which is inadequate to respond to a wide solar radiation flux. In order to improve on this design limitation, researchers have improved the nanostructuring [15-17] of the materials. This leads to a heterojunction of a size order close to the diffusion length, which in turn means all the exciton pairs can dissociate, like in fig.2c and d. Bulk Heterojunction has the best architecture for polymer solar cells, because exciton collection percentage is very high. A BHJ is formed by spin coating a solution from a polymer and an acceptor material. Common examples include mixes of P3HT or MDMO-PPV and fullerene derivatives, PCBM. By mixing the p-type and n-type materials (see Figure 2c) this ensures that each photogenerated exciton can lead to charge transfer because junctions are created throughout the bulk. Another successful implementation is the ordered heterojunction obtained generally by polymer infiltration in nanostructured oxide pores. TiO2 has the advantage here of being abundant and well-studied in the scientific community. Improved conversion efficiency can be achieved using gold nanoparticle (atomic deposition) on the indium tin oxide surface. These surface plasmonic gold nanodots can be engineered to absorb most of the [red-orange] light and can generate surface plasmon resonance. Coupling of the organic exciton and nanostructured plasmon allows a better charge transfer compared to the bulk heterojunction.

a.

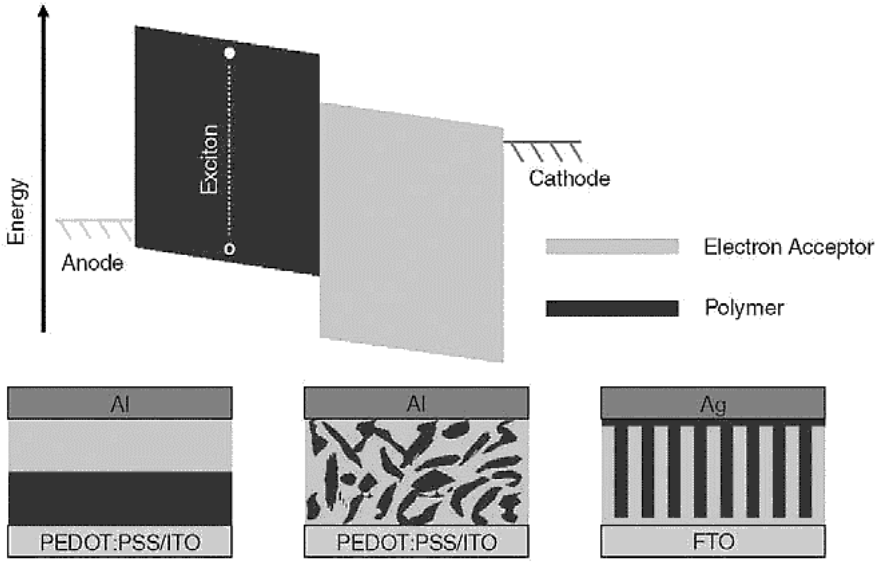

b. c. d.

Fig. 2. Polymer solar cell heterojunction architectures [18]:
a. energy diagram of a heterojunction (exciton in the polymer phase);
b. bilayer heterojunction (in this case the active layer must be thin for efficient exciton split);
c. bulk heterojunction;
d. ordered heterojunction.

3. **Materials and methods**

Considering the price per Watt and efficiency, the OPVs still have a long way to beat the polycrystalline silicon devices but emerging technologies and cheaper manufacture implementations make the organic solar cell a promising candidate for the clean, energy hungry future ahead. The state of the art implementation yields bandgap energies above or around 1.5eV and conversion efficiencies of 11.6% and 13.2% as reported by Yang Yang lab from UCLA and Heliatek spectively.

For an organic solar cell to perform efficiently, a selection of attributes must be optimized such as the p/n ratio, hole transport layer materials and the solvent system. Such materials (photoactive inks, fullerene derivatives and other molecules) are reported in the literature and available as subject to improvement. As a basic example of organic solar cell manufacturing, after all the materials have been chosen (including the PCMB:P3HT/ ICBA:P3HT photoactive ink and corresponding hole transport solution eg.S-P3MEET) the substrate is then prepared by ultrasonic cleaning in various solutions such as water and isopropyl.

Before the ink application the substrate also receives an *UV*/ozone treatment. Usually the solution deposition is done via spin coating on the appropiate calibration of the spin curve generated by the spin coater. Annealing the film after ink placement takes place at around 110-175°C for 15-30 minutes in air or inert atmosphere. Common practice for bulk heterojunctions is to use soluble low band gap polymers with high mobility, due to the fact that the V_{OC} depends on the LUMO of the acceptor and the HOMO levels of the donor. That is why, increasing the HOMO of the acceptor and/or lowering the LUMO of the donor is a sound design choice, effectively lowering the band gap.

Among molecular *p* type semiconductors, the most commonly used are: pentacene(P5), rubrene, molecular structures based on tiophene ring (6T, DH-6T, DH-4T, benzothiophene:BDT), copper phthalocyanine:CuPc, P3HT: poly-3-hexyl thiophene. Regarding *n*-type organic semiconductors, transport properties and structure correlation are still being explored.

There are two main methods of production. First consists of reduction treatment on the molecular orbital energy level via substitution with acceptor groups. Another is based on modifying the surface properties to control electron trapping. Examples include oligothiophenes modified by substitution with cyan, perfluoroalkyl/aryl and alkyl/arylcarbonyl groups, compounds based on naphthalene and perylene. Good mobility has been achieved for fullerene (C60) deposited on a monoatomic pentacene later and derivatives, like (PCBM) phenyl-C_{61}-butyric acid methyl ester. From available PCBMs, PCBM(Phenyl-C_{85}-Butyric-Acid-Methyl Ester) has the strongest visible absorption and highest electron accepting ability.

As stated by commercial sources (Plextronics, Solarmer), solutions and thin films are sensitive over time, changes in viscosity and film resistivity may be experienced beyond 6 month of storage under appropriate conditions (inert gas, 2-8 °C) before spin coating [7, 30]. However standardized methods for testing organic photovoltaics lifetime are still being evaluated. Well preserved devices can be stored stable for many months, but the ultimate lifetime is still relatively unknown.

The three parameters that govern the energy conversion efficiency in BHJ OPVs are the I_{sc}(short current), V_{oc}(open circuit voltage) and FF(fill factor). Typical values for V_{oc} fall between 0.4 and 0.8 volts, for I_{sc} between 5 and 15 mA/cm^2 and the FF is usually between 0.4 and 0.9. The fill factor (1) FF is a ratio to the ideal characteristics and is represented as seen below. The PCE(power conversion efficiency) is also used to compare devices.

$$FF = \frac{V_{\max} \cdot I_{\max}}{V_{OC} \cdot I_{SC}} \quad PCE = \frac{FF \cdot V_{OC} \cdot I_{SC}}{InputOpticalPower(W)} \tag{1}$$

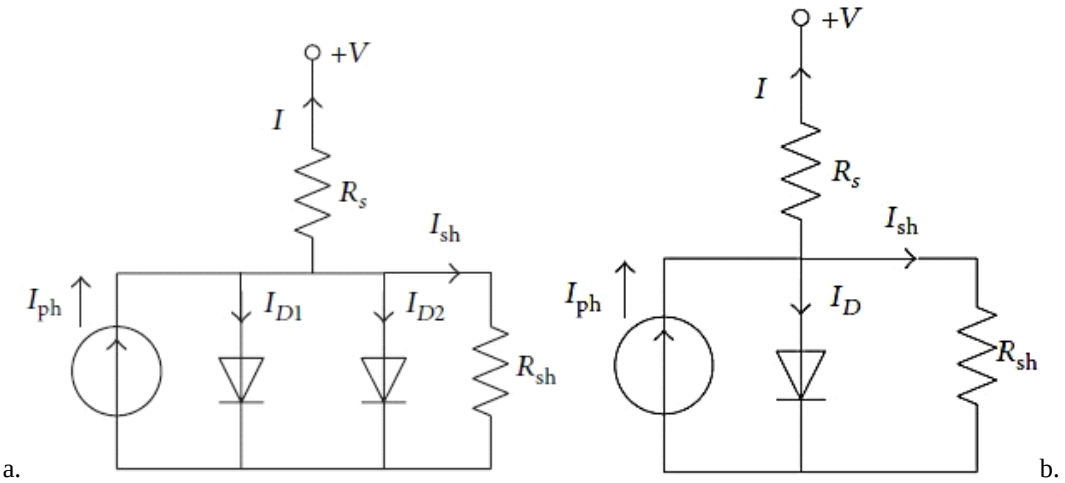

Fig. 3. Equivalent circuits of double(a) and single(b) diode models

Considering the similarities to the diode structure it is only natural that the most used methods of simulation make use of a single or double diode model. The latter is more exact but has 7 unknown parameters as opposed to the single diode model which has only 5. For the accuracy combined with simplicty the single diode model has been commonly used to validate experimental data. The representative circuits are shown below (see Figure 3).

The R_s and R_{sh} represent the series and shunt resistances and signify the imperfection of the solar cell vs the ideal model and are harder to calculate. In the case of single diode approximation the model can be written as follows:

$$I = -I_{ph(photogenerated)} + I_{d(diode)} + I_{sh(shunt)} \tag{2}$$

$$I = -I_{ph} + I_0(\exp[\frac{V + IR_s}{nK_BT/q}] - 1) + (V + IR_s)\frac{1}{R_{sh}}, 1/R_{sh} -> G_{sh}, K_BT/q -> V_{th} \tag{3}$$

with I_0 being the reverse saturation current, G_{sh} the shunt conductance, V_{th} thermal voltage and n the ideality factor.

The first algorithm (*Lambert function model*) should yield precise results as it uses an analytical solution circumventing numerical approximation unlike the other algorithms but is more computationally intensive. The second algorithm (*double fit model*) should be faster and flexible, but the complicated part is branching out the two parts of the curve for the different fit. However this model is considered to be more flexible than the others even if it is expected to have lower accuracy versus the analytical solution. The third algorithm (*linear regression model*) is independent of the voltage step and should provide decently accurate parameters.

4. **Results and discussion**

OPVs represent a field in constant evolution and rapid development, therefore precise, reliable parameter extraction is required alongside. The experimental values were obtained thanks to University of Waterloo and from digitized literature data [18, 19] and displayed in Figure 4.

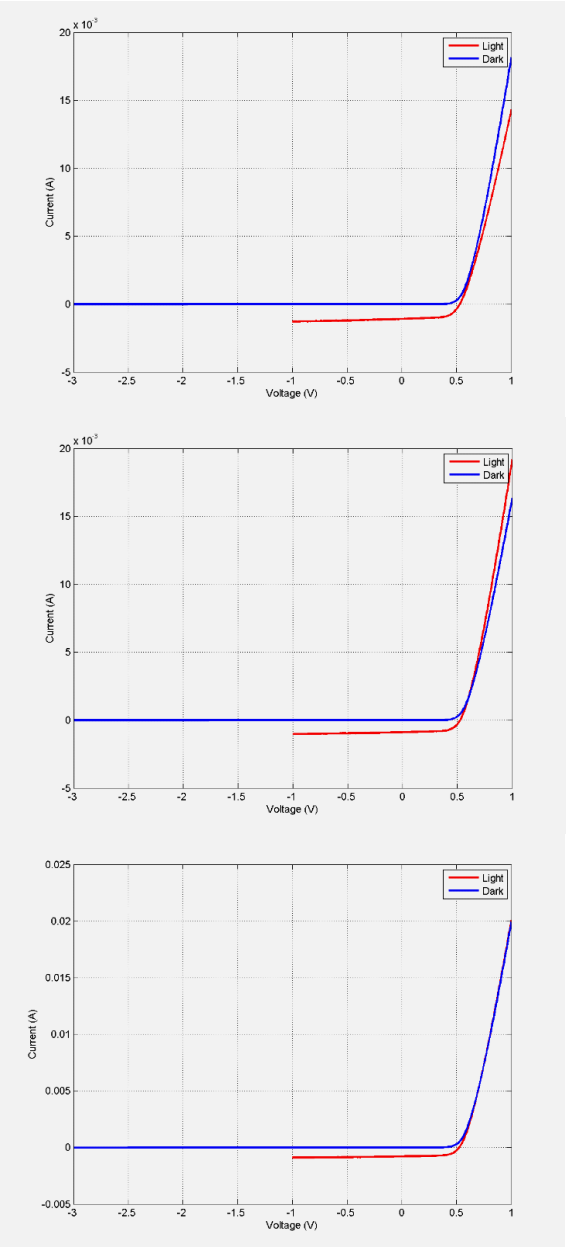

Fig. 4. Characteristics from the output data used for the parameter extraction methods.

As investigation and diagnostics tool, the simulated methods of parameter extraction are fine but they perform clearly different from a precision and performance standpoint. *Lambert function model* [3] is straightforward and based on nonlinear least squared error fit on the single diode model equation above, which is hard to solve explicitly due to the exp function inside. Lambert W function is used instead. This algorithm can suffer divergence and uses a greater amount of resources but yields precise results. *Double fit model* [4, 5, 20] rewrites conveniently the same diode model equation to extract and replace the voltage with the current inside the brackets. The logic behind it is to approximate separately one part of the IV curve linear and the other one as an exponential. After the linear branch fit, a least squares method is then executed for the exponential fit to reveal the solar cell parameters. This method is faster and exhibits accurate parameters provided the branching out the two parts of the curve for the different fit is done properly. *Linear regression model* compared [6,27] presents a linear regression on a derivation from the raw OPV experimental data. The drawback of this function is that its output is not consistent when subjected to a wide range of *I-V* data, and so it the farthest from convergence among the algorithms tested. However, satisfactory agreement was obtained for all methods (see Table 1), when the behavior of the solar cell was within bounds to the diode model, literature reports divergence increases at lower temperatures and discrepancies have been observed to increase in such conditions. The residual sum of squares was calculated with the help of Lambert w functions, used to predict the current versus the experimental data [3]. The error function takes the input data together with initial guess values for the ideality factor, reverse saturation current and series resistance. Discrepancies between the experimental data and the estimation were rather low, when evaluated with sum of squared errors of prediction, respectively (SSE 0.0145, 0.0197, 0.0274).

Table 1. OPV parameters obtained according to the three models [3-6, 12]

Analyzed model	***Lambert function model***			***Double fit model***			***Linear regression model***	
I_{sc} (A)	*Data 1*	*Data 2*		*Data 1*	*Data 2*		*Data 1*	*Data 2*
	0.000792	0.000889		0.001091	0.000739		0.000784	0.001135
J_{sc} (mA/cm^2)	3.958625	4.44745		5.452725	3.694075		3.920375	5.676175
V_{oc} (V)	0.525	0.525		0.53	0.52		0.52	0.53
FF	0.650773	0.655608		0.627731	0.654749		0.647976	0.636638
R_{series} (Ohm·cm^2)	72.36655	4.660882		14.92057	22.89531		50.09785	5.013329
R_{shunt} (Ohm·cm^2)	1413.159	796.9799		719.4514	1818.329		1399.696	715.9908
n	2.253812	5.156421		4.346715	3.86362		3.018765	4.884659
J_0 (mA/cm^2)	6.88E-05	0.068803		-0.03278	0.011299		-0.00094	0.069836
PCE (%)	1.352488	1.530786		1.814107	1.25772		1.32096	1.915246

The emerging techniques that combine new algorithms give better results towards error mitigation and precision, as can be seen in the use of artificial bee swarm optimization algorithm ABSO [21] or the mutative-scale parallel chaos optimization algorithm MPCOA [22]. As a sure, future improvement of these methods, the wide adoption of heuristics, neural network or fuzzy logic algorithms is required [23-25].

5. **Conclusions**

This work presents a theoretical analysis for three different algorithms used for parameter extraction from raw *I-V* data corresponding to an illuminated organic solar cell. The nonlinear fitting techniques together with the discussed analytical models are in good agreement with the literature. Such methods provide a solid base for comparison and device evaluation however the models themselves are subject to conditions that sometimes affect the crucial precision required, for a wide selection of input values.

R E F E R E N C E S

[1] A. M. Bagher, *Comparison of organic solar cells and inorganic solar cells*, International Journal of Renewable and Sustainable Energy 3, pp. 53-58, **2014**.

[2] M. R. Mitroi, L. Fara, and M. L. Ciurea, *Numerical procedure for optimizing dye-sensitized solar cells*, Journal of Nanomaterials 2014, p. 27, **2014**.

[3] A. Jain and A. Kapoor, *A new approach to study organic solar cell using Lambert W-function*, Solar Energy Materials and Solar Cells, vol. 86, pp. 197-205, **2005.**

[4] M. Chegaar, et al., *Simple parameter extraction method for illuminated solar cells*, Solid-State Electronics, vol. 50, pp. 1234-1237, **2006**.

[5] K. Bouzidia, et al., *Solar cells parameters evaluation considering the series and shunt resistance*, Solar Energy Materials and Solar Cells, vol. 91, pp. 1647-1651, **2007**.

[6] N. Nehaoua, et al., *Determination of organic solar cell parameters based on single or multiple pin structures*, Vacuum, vol. 84, pp. 326-329, **2009.**

[7] Rogojan, Rodica, et al. "Spectral behavior and nonlinear optical properties of aluminophosphate semiconductor-doped glasses." *11th International School on Quantum Electronics: Laser Physics and Applications*. International Society for Optics and Photonics, **2001**.

[8] A. Serbenta, et al., *Bulk Heterojunction Morphology of Polymer:fullerene Blends Revealed by Ultrafast Spectroscopy*, Sci. Rep. 6, 36236, **2016**.

[9] N. K. Elumalai and A. Uddin, Open circuit voltage of organic solar cells: an in-depth review, Energy Environ. Sci., 9, pp. 391-410, **2016**.

[10] P. Sterian, Photonics , 580 p., Printech, Bucharest, **2000.**

[11] H. Huang, J. Huang, Organic and hybrid solar cells, 337 pp., Chapter 2, Springer, **2014**.

[12] V. Coropceanu et al., *Charge transport in organic semiconductors*, Chem. Rev., 107(4), pp. 926-952, **2007**.

[13] K. Feron, et al., *Organic Solar Cells: Understanding the Role of Förster Resonance Energy Transfer*, Int. J. Mol. Sci. 13(12), pp. 17019–17047, **2012**.

[14] I.G. Scheblykin et al., *Excited State and Charge Photogeneration Dynamics in Conjugated Polymers*, J. Phys. Chem. B 111 (23), pp. 6303–6321, **2007**.

[15] J-T. Chen and C-S. Hsu, *Conjugated polymer nanostructures for organic solar cell applications*, Polym. Chem., 2, pp. 2707-2722, **2011**.

[16] Y-S Cheng and C. Gau, *Efficiency improvement of organic solar cells with imprint of nanostructures by capillary force lithography*, Sol. Energ. Mat. Sol. Cells, vol. 120 B, pp. 566-571, **2014**.

[17] C-Y. Nam et al., *Nanostructured electrodes for organic bulk heterojunction solar cells: Model study using carbon nanotube dispersed polythiophene-fullerene blend devices*, J. Appl. Phys., vol. 110 064307, **2011**.

[18] A. C. Mayer et al., *Polymer-based solar cells*, Materials Today, vol. 10, issue 11, **2007**.

[19] www.eng.uwaterloo.ca/~g3willia.

[20] Z. Ouennoughi and M. Chegaar, *A simpler method for extracting solar cell parameters using the conductance method*, Solid-State Electronics, vol. 43, pp. 1985-1988, **1999.**

[21] A. Askarzadeh, A. Rezazadeh, *Artificial bee swarm optimization algorithm for parameters identification of solar cell models*, Appl. Energy, vol. 102, pp. 943-949, **2013**.

[22] X. Yuan et al., *Parameter extraction of solar cell models using mutative-scale parallel chaos optimization algorithm*, Solar Energy**,** vol. 108, pp. 238-251, **2014**.23.

[23] A. Sterian, P. Sterian, *Mathematical Models of Dissipative Systems in Quantum Engineering*, Mathematical Problems in Engineering, vol. 2012, Article ID 347674, 12 pages

[24] D. Gotleyb et al., *Characterisation and Modeling of Organic Solar Cells by Using Radial Basis Neural Networks*, ICAIASC 2016: Artificial Intelligence and Soft Computing, pp. 91-103, **2016**.

[25] A. Laudani et al., *Hybrid Neural Network Approach Based Tool for the Modeling of Photovoltaic Panels*, Int. J. Photoenergy, vol 2015, 10 pages, **2015**.

[26] Popescu I.M. et al., *Applications of Lasers* (in Romanian), 521 pp., Technical Publishing House, **1979**.

[27] Sterian, Paul E. *Transmisia optica a informației*, Editura Tehnică, **1981**.

[28] Fara, Silvian et al., *New Results in Optical Modelling of Quantum Well Solar Cells. International Journal of Photoenergy*, **2012.**

[29] Iordache, Dan-Alexandru, et al. *Complex computer simulations, numerical artifacts, and numerical phenomena*, International Journal of Computers Communications & Control 5.5 (**2010**): 744-754.

[30] Sigma-Aldrich Co. LLC, Technical Bulletin, **2012.**